



## Analysis of Heat Potential in Solar Panels for Thermoelectric Generators using ANSYS Software

Catur Harsito <sup>1\*</sup>, Teguh Triyono <sup>1</sup>, Eki Rovianto <sup>1</sup>

<sup>1</sup>Department of Mechanical Engineering Universitas Sebelas Maret, Surakarta, Indonesia.

Received 27 April 2022; Revised 21 June 2022; Accepted 29 June 2022; Published 01 July 2022

### Abstract

The growing demand for energy has an impact on the development of environmentally friendly renewable energy. The sun is energy that has the potential to be used as electrical energy through light energy and heat energy. Recently, research interest related to photovoltaic performance has increased. Several studies have investigated the effect of panel cooling on photovoltaic performance. In this study, the use of exergy solar panels is considered to improve performance by adding a thermoelectric system. Research work related to photovoltaic testing with thermoelectrics at low temperatures has not been carried out. Therefore, experimental methods to obtain temperature profiles and simulation methods to see the power potential generated from thermoelectrics have been carried out. The experimental method is carried out using monocrystalline panels with type K sensors to retrieve temperature data and data acquisition as deviations from the current, voltage, and temperature results of the panel. The simulation model was carried out using the ANSYS software. Tests are carried out, taking into account the effect of back panel temperature on system performance. The results showed that the photovoltaic temperature fluctuated due to the influence of cloud cover, the highest photovoltaic temperature was 57°C, and the lowest temperature was 30°C. The maximum power produced by photovoltaic is 39.8W. It is then applied to the thermoelectric simulation based on the highest temperature, and the maximum power value is 1673.4 mW. This photovoltaic-thermoelectric generator system produces a 4.2% increase in power value over conventional photovoltaic systems. The findings in this study can be used as a reference for all types of low-temperature photovoltaic-thermoelectric systems.

*Keywords:* Photovoltaic-Thermoelectric Generator; FEM; Renewable Energy; Heat Potential.

### 1. Introduction

The increasing energy demand impacts the development of renewable energy, green energy, and environmentally friendly energy due to the depletion of natural resources. Several renewable energy sources, such as wind energy and hydro energy, have also been used [1–3]. Solar energy has a very large energy source. The potential forms of energy to be used as electrical energy from the sun are light energy and heat energy. Solar panel devices can directly generate electrical power by converting sunlight energy into electricity. The heat energy that arises affects the efficiency of the solar panels and is the main weakness of this device. An increasing solar panel temperature can reduce its performance.

The waste heat from the solar panel module can be used as an energy source without mechanical components using a thermoelectric generator. This thermoelectric generator has many advantages because it has advantages as a photovoltaic system with a static thermal structure, lasts for years, and is completely quiet and clean [4]. A thermoelectric generator is a solid-state device that utilizes the Seebeck Effect to generate electrical energy from thermal energy due to the difference in temperature on both sides [5–7]. A study related to the utilization of waste energy with a TEG system

\* Corresponding author: [catur\\_harsito@staff.uns.ac.id](mailto:catur_harsito@staff.uns.ac.id)

 <http://dx.doi.org/10.28991/CEJ-2022-08-07-02>



© 2022 by the authors. Licensee C.E.J, Tehran, Iran. This article is an open access article distributed under the terms and conditions of the Creative Commons Attribution (CC-BY) license (<http://creativecommons.org/licenses/by/4.0/>).

has been carried out. The heat energy in the vehicle exhaust is utilized by adding thermoelectric devices, some even add a cooling system to maximize output performance [8]. Three-dimensional numerical studies on thermoelectrics have been carried out to determine the temperature profile and determine the performance of the thermoelectric [9]. Suzuki also investigated the combination of heat transfer from thermoelectric to free fluid to see the phenomenon that occurred [10]. In addition, the application of thermoelectrics is also commonly combined with other systems, which are commonly referred to as hybrid systems. The hybrid system is one solution to increase the efficiency of solar panels. Several hybrid systems have been studied recently [11–13].

The discussion related to the combination of Photovoltaic-Thermoelectric generator technology has been carried out critically and has proven to be an alternative energy source through light energy and solar thermal energy, which results in increased output efficiency. Thermoelectric generators have been reviewed in recent years [14–16]. This combined system has been implemented with many configurations, physically integrated or separate. In general, the combination is done by placing or attaching the TEG to the back of the PV panel by separating the solar photon energy that cannot be absorbed by the PV-TEG using a spectrum splitter. [17–19]. This system has the advantage of having two systems combining the output power produced will be greater. The addition of the system or modification of the PV-TEG configuration is carried out to optimize the output power. The total output power of this hybrid system is the sum of the power of the PV module and TEG module. Hybrid systems have also been applied to vehicle exhausts [8] and telecommunications systems [20].

This study aimed to verify the daily heat potential generated from solar panels to generate electricity using a thermoelectric module. This Hybrid Photovoltaic with a thermoelectric generator utilizes excessive heat in the solar panel by connecting a thermoelectric generator on the bottom side of the panel. Furthermore, this heat distribution characteristic is used as a reference for laying the thermoelectric position to produce maximum power. The electric power potential on the thermoelectric is applied to a 3D simulation and solved using the finite element method. The results show that photovoltaic heat can be used as a thermoelectric input and increase power in a hybrid system.

## 2. Methods

This study used experimental methods to produce the temperature distribution at the top and bottom of the panel, then used as heat input for the simulated thermoelectric generator module. The solar panels are conditioned to resemble the roof of a house with a slope of 20 degrees [21]. This replica of the roof of this house is placed in an open rooftop area close to the six engineering faculties building, Universitas Sebelas Maret (7°33'49.1"S 110°51'19.0"E), Indonesia (Figure 1). Figure 2 shows the flowchart of the research methodology and Figure 3 shows the experimental configuration.



Figure 1. Location of the study area

The solar panel used in this research is Mono-crystalline type, with dimensions 540×670×30mm, Rated Maximum Power ( $P_m$ ) = 50W, Voltage ( $V_{mp}$ ) = 18V, Current ( $I_{mp}$ ) = 2.78A, Open-Circuit Voltage ( $V_{oc}$ ) = 22.4V, Short-Circuit Current ( $I_{sc}$ ) = 3.24A. Above and below the panel, ambient temperature data were taken using a K-type thermocouple sensor attached to the surface. Solar radiation is measured using a solar power meter (Lutron SPM-1116SD).

The absorption of solar energy and temperature distribution on the solar panels installed on the house's roof was analyzed. The characteristics of the heat generated at the bottom of the panel are then used as a heat source for the thermoelectric generator. The potential of electrical energy generated by the thermoelectric generator is simulated with

ANSYS software. The schematic diagram of the thermoelectric generator can be seen in Figure 4. The size of the thermoelectric generator used is 40×40 mm in length, with material properties shown in Table 1 [10, 22, 23]. While the value of Thermal Conductivity (k) and Seebeck Coefficient (S) in Bi2Te3 is determined using the formula below.

$$k = 4E-05T^2 - 0.0233T + 4.4964 \tag{1}$$

$$S = 2E-09T^2 - 2E-06T + 6E-05 \tag{2}$$

$$\sigma = (1.56E-02T^2 - 15.708T + 4466.38) \times 10^2 \tag{3}$$

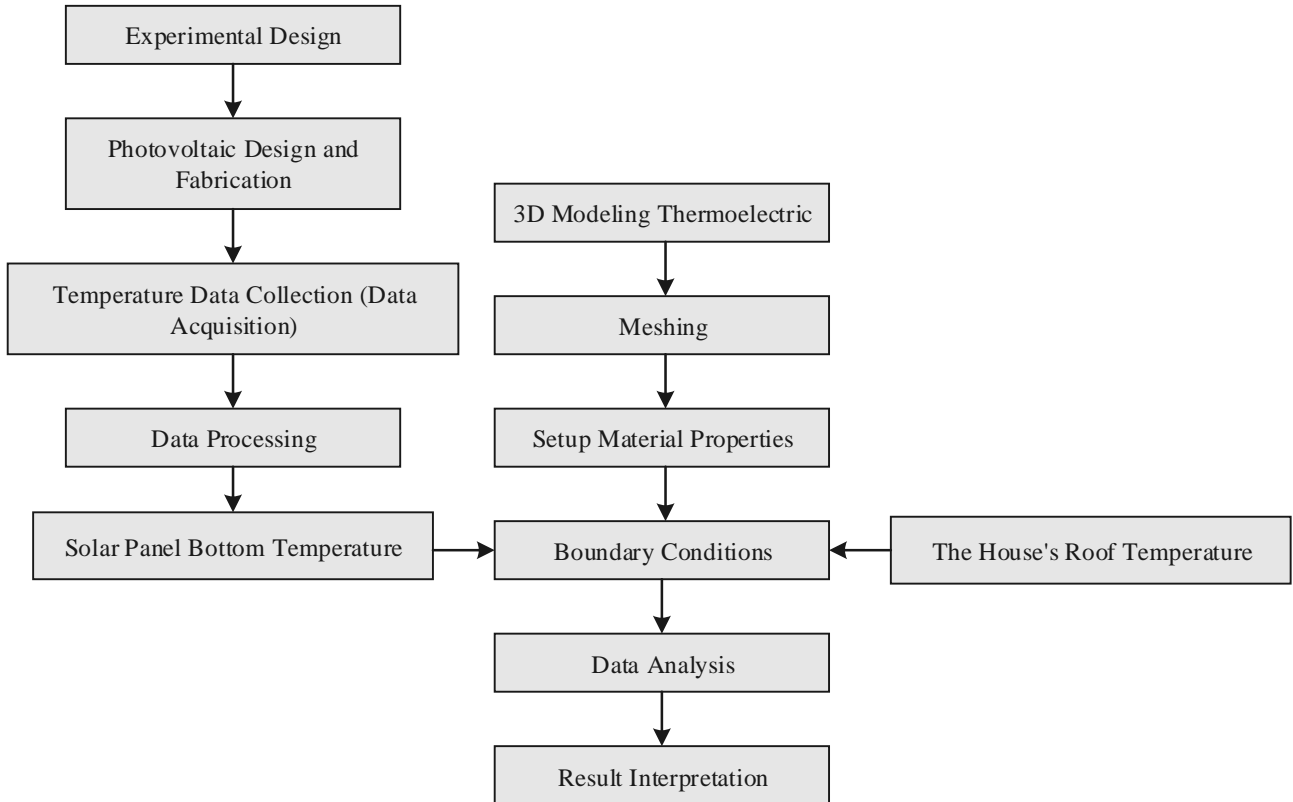


Figure 2. Flowchart of the research methodology

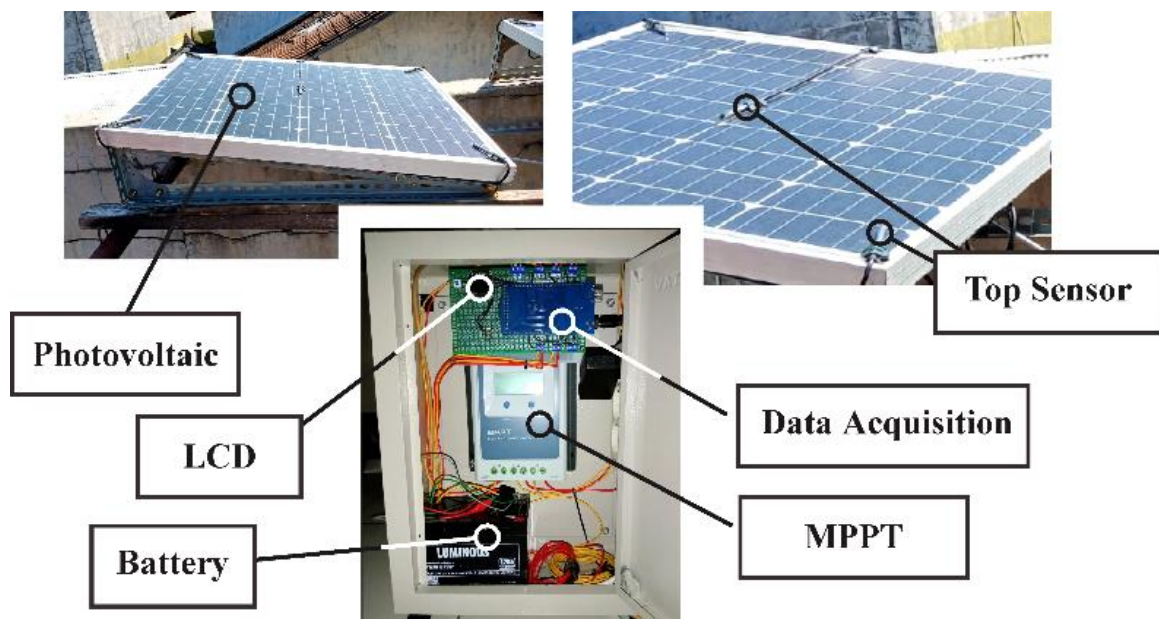


Figure 3. Experimental setup

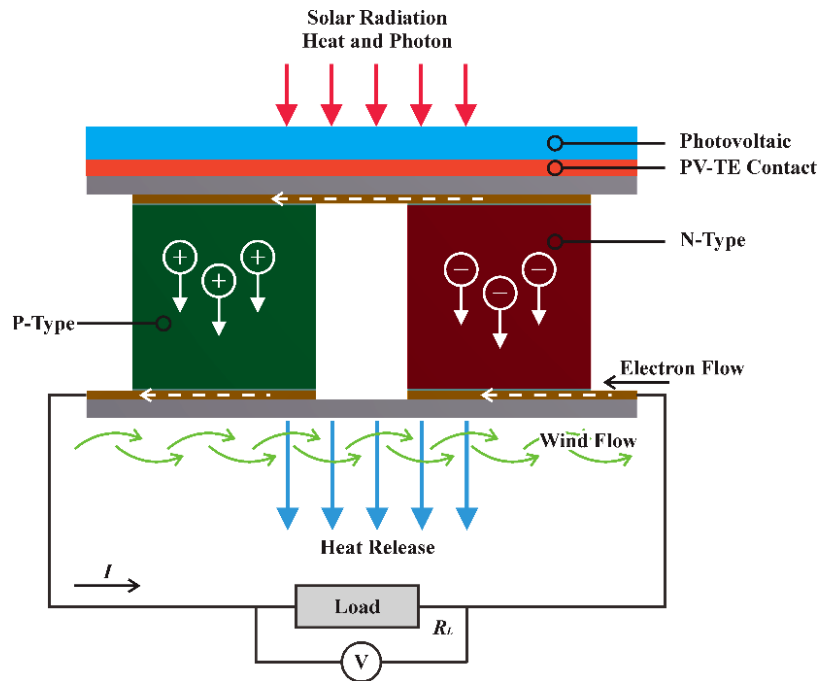


Figure 1. Schematic diagram of the thermoelectric generator

Table 1. Material properties

Material	$k$ (W/m K)	$S$ ( $\mu\text{V/K}$ )	$\sigma$ (S/m)
Al <sub>2</sub> O <sub>3</sub>	36	-	-
Bi <sub>2</sub> Te <sub>3</sub> -	-(1)	(2)	(3)
Bi <sub>2</sub> Te <sub>3</sub> +	(1)	(2)	(3)
Cu	398	1.83	640
SnPb	20	-	-

### 2.1. Modeling of Thermoelectric Generator

Modeling of thermoelectric using ANSYS software. Modeling and analyzing the thermoelectric characteristics of the generator is simplified. The thermoelectric module is composed of 4-legs. Figure 5 shows the characteristics of the thermoelectric elements used for the simulation. The p-type elements are shown in green and the n-type elements are in red, both connected together with a 0.3 mm series connector. The splicing material between copper and p-type/n-type elements is SnPb. The top and bottom surfaces are covered with 0.8mm thick Al<sub>2</sub>O<sub>3</sub> ceramic. The single element size of the thermoelectric is 10×10×10 mm with a distance between elements of 5 mm. The size of the thermoelectric module is 30×30×13 mm. Modeling and analyzing the thermoelectric characteristics of the generator is simplified. The boundary conditions in the FEA modeling are determined by considering the TE power plant utilizing PV panel heat. In this paper, the photovoltaic bottom temperature data is used as a thermoelectric numerical evaluation. These data are assumed to be on the hot side and on the cold side is 24°C which is the ambient temperature. The convection coefficient is assumed to be 1E-6 W/m<sup>2</sup>°C as the TE surface insulation condition. The electric potentials of 0.087V (P-leg side) and 0V (N-leg side) are applied to analyze the power plant. This boundary condition is shown in Figure 6.

### 2.2. Validation

In every numerical modeling used in system analysis, validation is always conducted. It is a traditional practice to remove all doubts about the accuracy of the results obtained. The validation method used is the current numerical model approach to reproduce the results of previous research works. As proof that the model made is indeed accurate, validation tests were conducted with a 4-leg model which is similar to the following dimensions: leg height 3mm; leg width 1.4mm; leg length 1.4mm; spacing between legs 1mm; conductor thickness 0.15; substrate thickness 0.8mm; and solder thickness 0.1mm [24]. The accuracy of the resulting numerical modeling depends on the validation process, the validation process is said to be accurate if it produces a value similar to the results of a verified paper published. This model can be used as a basis for predicting thermoelectric performance with different leg sizes. The results of the validation test are shown in Table 2. The validation results show a slight difference but have a minimal error value below

0.5%. Based on the validation results, it can be concluded that there is a similarity between the results obtained from this numerical modeling and the paper previously published by Erturun 2012. So it can be concluded that the model used in this study is considered accurate and reliable for predicting numerical modeling of photovoltaic-thermoelectric generator performance. In the validation section, the meshing adjustment used also affect the results of parametric solving using ANSYS software. This adjustment involves increasing the size of the mesh elements until the output matches the previous paper. This test states that the results obtained are appropriate with the very fine meshing size. The meshing results are shown in Figure 7, where meshing uses the hexagonal method 5 by making more detailed settings on parts that have a small size to get the distribution results.

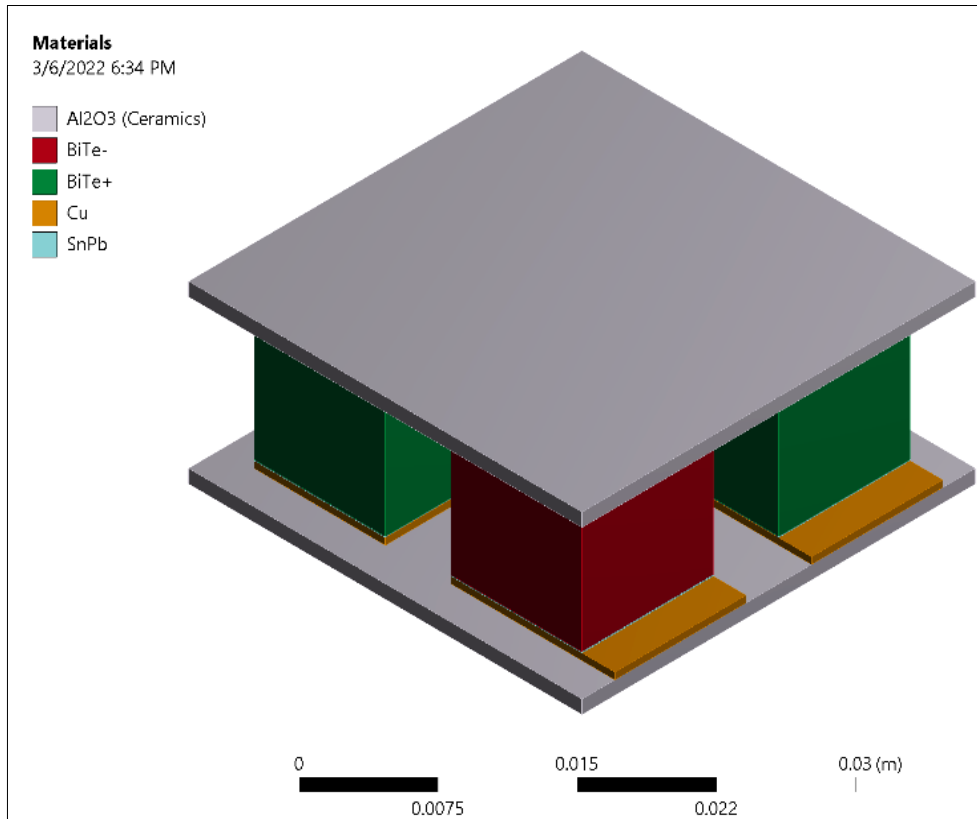


Figure 2. Thermoelectric model

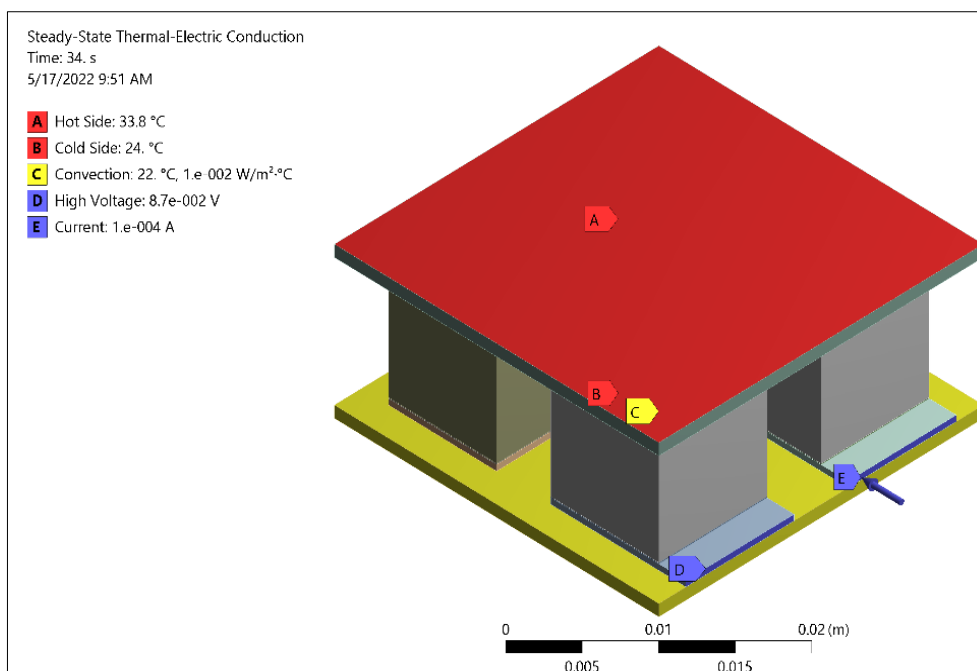
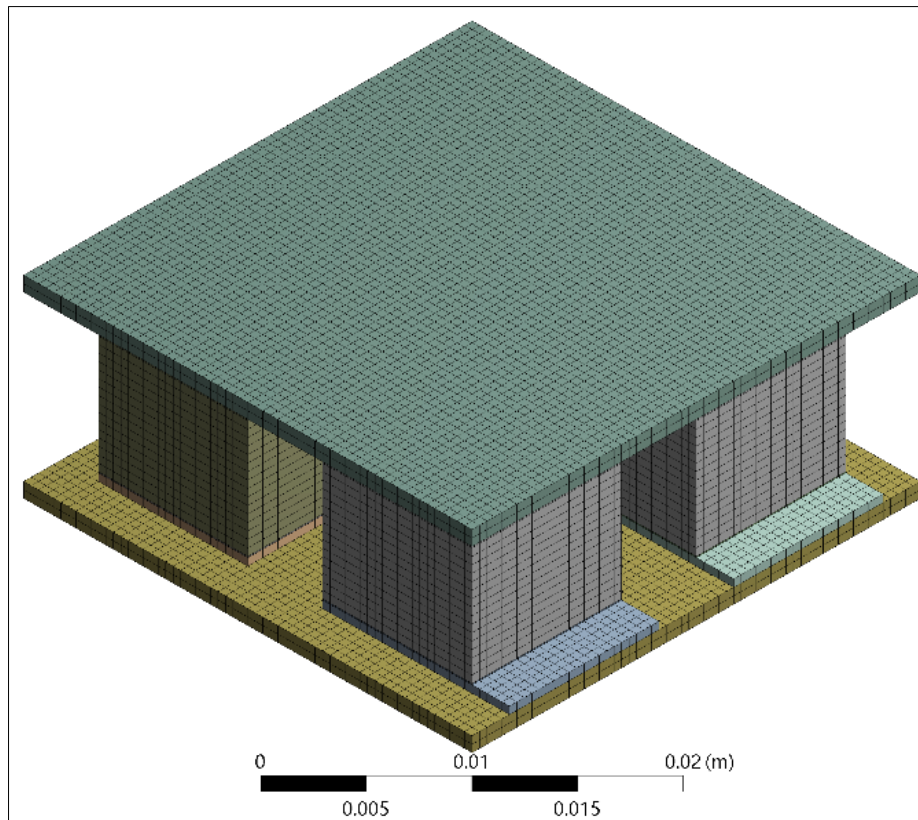


Figure 3. Boundary condition

**Table 2. Simulation Validation**

Variable	Erturun 2012	Validation	Error (%)
Current Generated (mA)	328	326.85	0.35%
Heat Absorbed (mW)	673	672.95	0.01%
Power Output (mW)	28.5	28.4	0.22%
Efficiency	4.24	4.23	0.34%

**Figure 4. Meshing Model**

### 3. Result

This section presents and discusses the experimental results and numerical analysis resulting from the proposed modeling. Photovoltaic performance is monitored for one full day to get the average energy produced. Furthermore, the thermoelectric performance is modeled at low temperatures as a result of experimental monitoring analysis. The evaluated thermoelectric performance is the distribution of temperature, electric voltage, and power generator.

#### 3.1. Photovoltaic Power Generator

Monitoring of daily temperature and light intensity is provided in a time range of 7.30-16.00 (GMT+7) every 15 minutes. These results are shown to see the potential heat that occurs in the hybrid solar panel and thermoelectric generator system as the maximum utilization of solar energy. The monitoring results are selected at certain times with a time range of 7.30-16.00 (GMT+7) with 15-minute intervals, and the light intensity is presented in Figure 8. Panel bottom temperature ( $T_b$ ) increases with time and decreases after 13.00 (GMT+7). The highest temperature obtained was  $57^{\circ}\text{C}$  at 13.00 (GMT+7), and the lowest temperature was  $30^{\circ}\text{C}$  at 7.30 (GMT+7). During the data collection range, the bottom panel temperature fluctuated. The temperature dropped at 10.15 (GMT+7), then rose gradually and decreased at 10.45 (GMT+7), rising again at 12.30 (GMT+7). This increase and decrease are influenced by white clouds covering the panel (shadow). This also occurs at the maximum temperature of the solar panels ( $T_a$ ). Meanwhile, the temperature under the panel (ceiling) is considered constant, then used as an input parameter for the thermoelectric generator. The effect of fluctuations in temperature readings caused by changes in the weather is proportional to fluctuations in the sun's intensity [19, 25]. This fluctuation also affects the output voltage generated by the thermoelectric generator.

Figure 9 shows the electrical power monitoring from Photovoltaic taken for four days, from 7.30 to 16.00. The value of the resulting power fluctuates according to the intensity and the existing temperature. The maximum power value is obtained at 39.8W

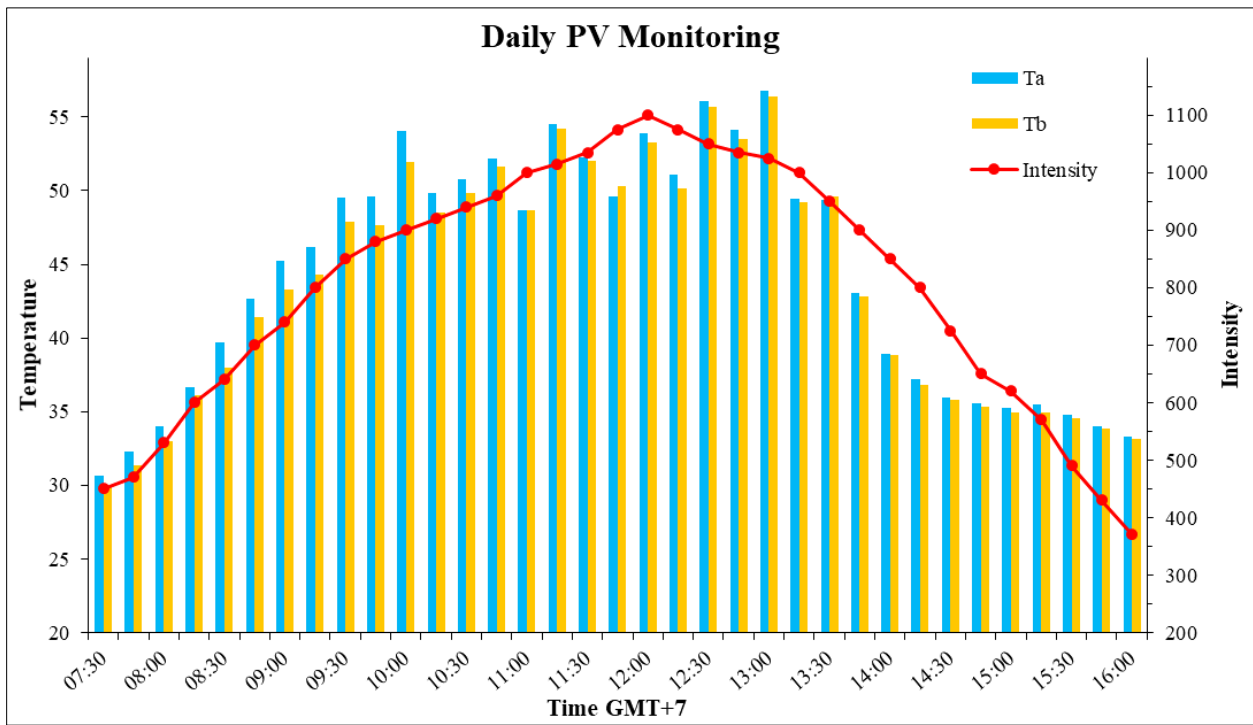


Figure 5. Daily panel temperature

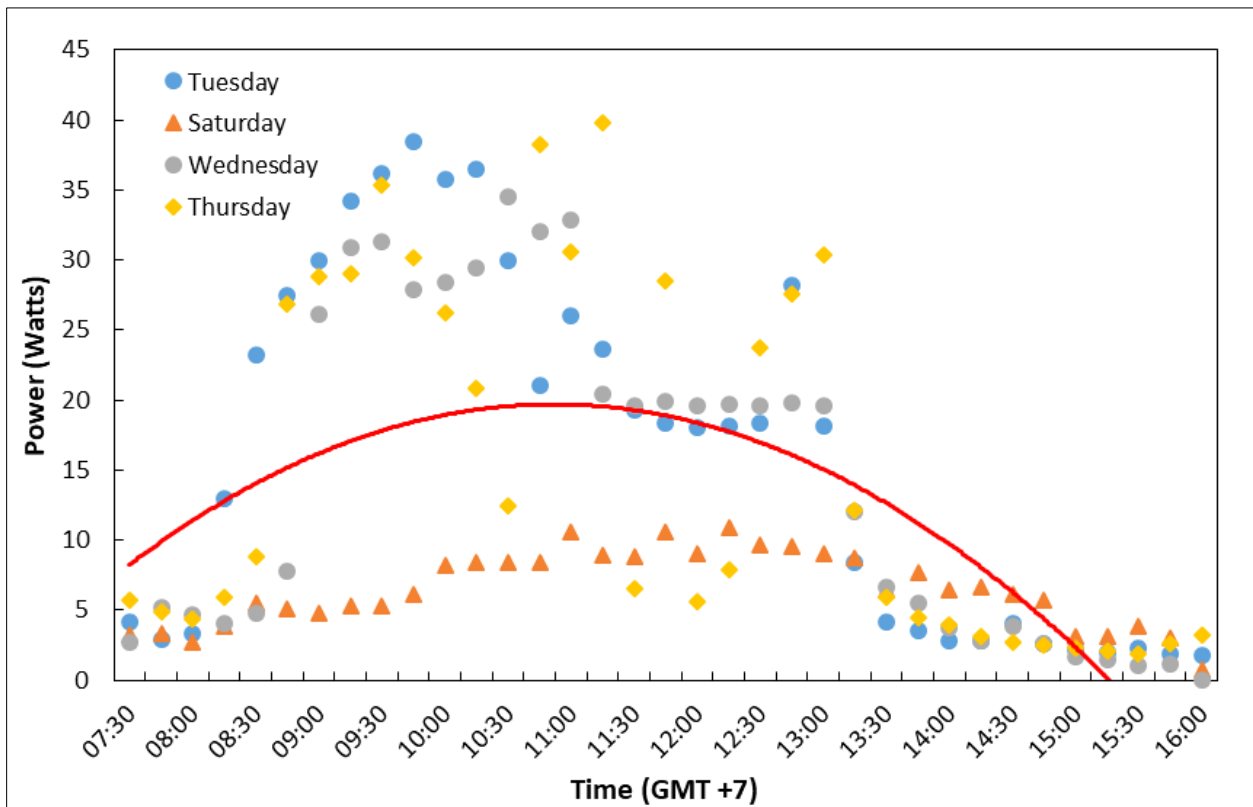


Figure 6. The power generator of Photovoltaic

### 3.2. Thermoelectric Power Generation

After doing the finite element method analysis, the results of the temperature distribution on the thermoelectric model are shown in Figure 10. Some experimental data are used as input. In this case, the thermoelectric top heat simulation is the daily bottom panel temperature data. The temperature on the top surface of the copper showed a homogeneous result, namely 56.4°C. The more homogeneous surface temperature of the copper electrode shows that the ceramics layer with a thickness of 0.8 mm at the top has a high effectiveness as a conductor of heat along the horizontal direction, this result is in line with articles published in previous journals.

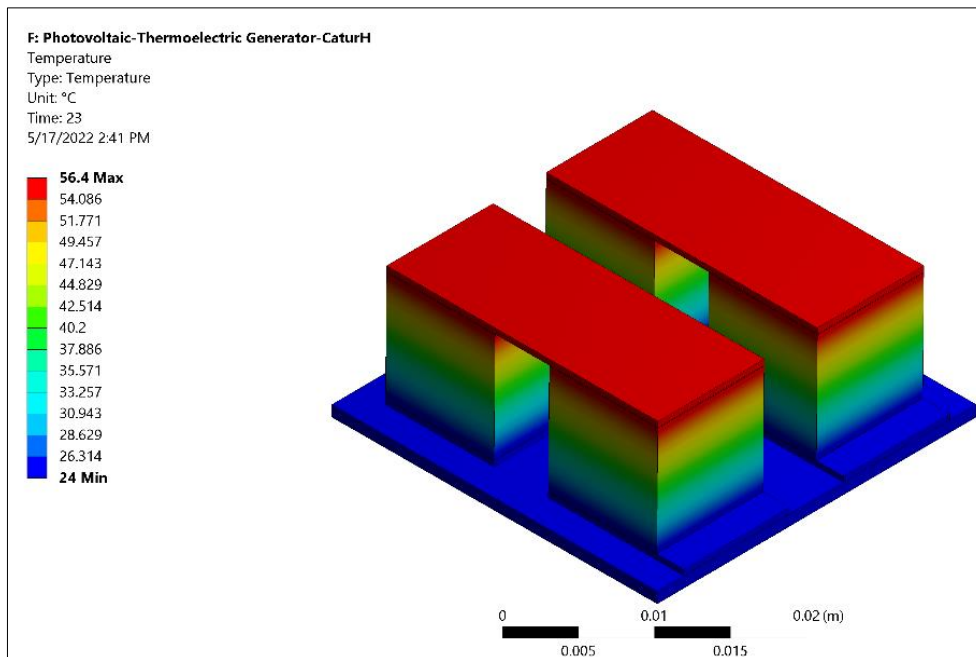


Figure 7. Temperature distribution on maximum output power generated

Linear temperature changes are seen in the thermoelectric leg area due to steady-state conditions. According to the literature, the temperature distribution on this thermoelectric leg experiences linearly [26, 27]. The cold side surface temperature shows a value of 34°C; the cold side is kept constant to extract the input heat effectively. The low-temperature difference on both sides of the thermoelectric does not affect the distribution of the leg material. This linear temperature profile was obtained due to the homogeneous temperature distribution in the hot ceramics layer. The assumption of the SnPb adhesive layer does not have a big impact on the difference in the effectiveness of the temperature distribution, because the temperature difference between the hot and cold side shows small results.

The thermoelectric output is obtained by connecting an external load. Voltage and power values can be generated by clicking an external load to the thermoelectric circuit. Multiplication of the current and the voltage across the two external terminals gives the power value. The distribution of electric voltage output at the highest value of 0.115V at 12.30 PM. The distribution profile of the electric potential increases linearly as shown Figure 101, and this potential is independent of the temperature generated in this test. This electric potential distribution profile is due to the Seebeck Effect. In addition, the effect of the adhesive layer does not significantly reduce the current in the circuit due to its low electrical resistivity.

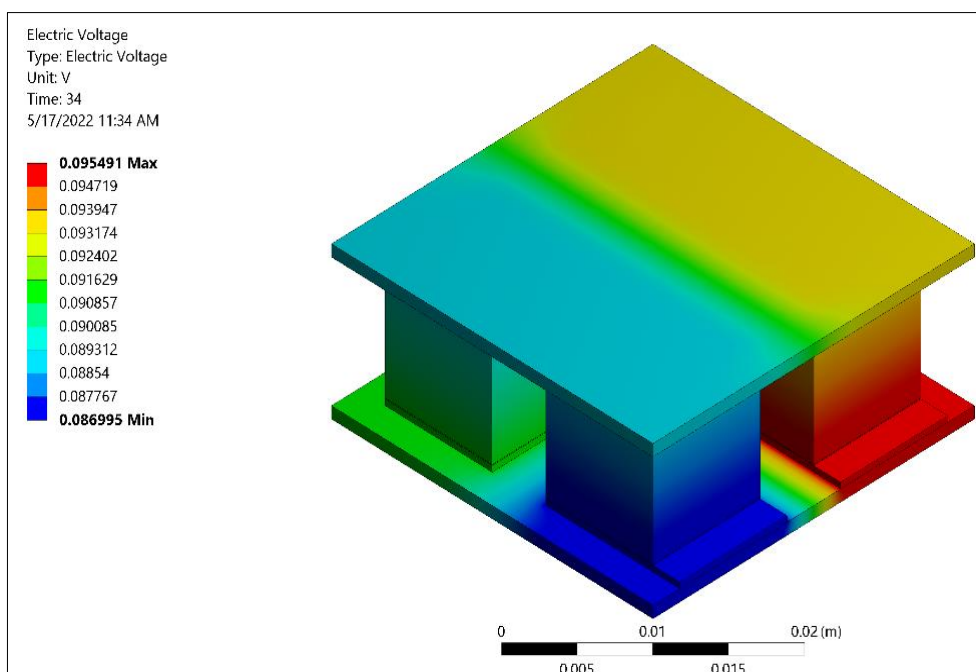


Figure 8. Electric Voltage

### 3.3. Photovoltaic-Thermoelectric Generator

The electricity potential generated by the thermoelectric for eight hours is described in this section. All-day simulations were applied to the thermoelectric using the ANSYS software. Figure 12 shows the simulation results of 8 hours Photovoltaic-Thermoelectric Generator system. The input temperature on the thermoelectric is the temperature value under the panel. The output power results show the maximum value at 12.30 PM, a common phenomenon in thermoelectric power generation systems. The results show that the power value increases at 10.45 and decreases when the panel temperature decreases at 01.00 AM, with the highest value of 1673.4 mW. In actual conditions, the value of the photovoltaic-thermoelectric generator is the result of the sum of the photovoltaic power values with the thermoelectric generator installed according to the photovoltaic area. The Photovoltaic Thermoelectric Generator system produces a value of 41.4734 W, an increase of 4.2% over conventional photovoltaic systems.

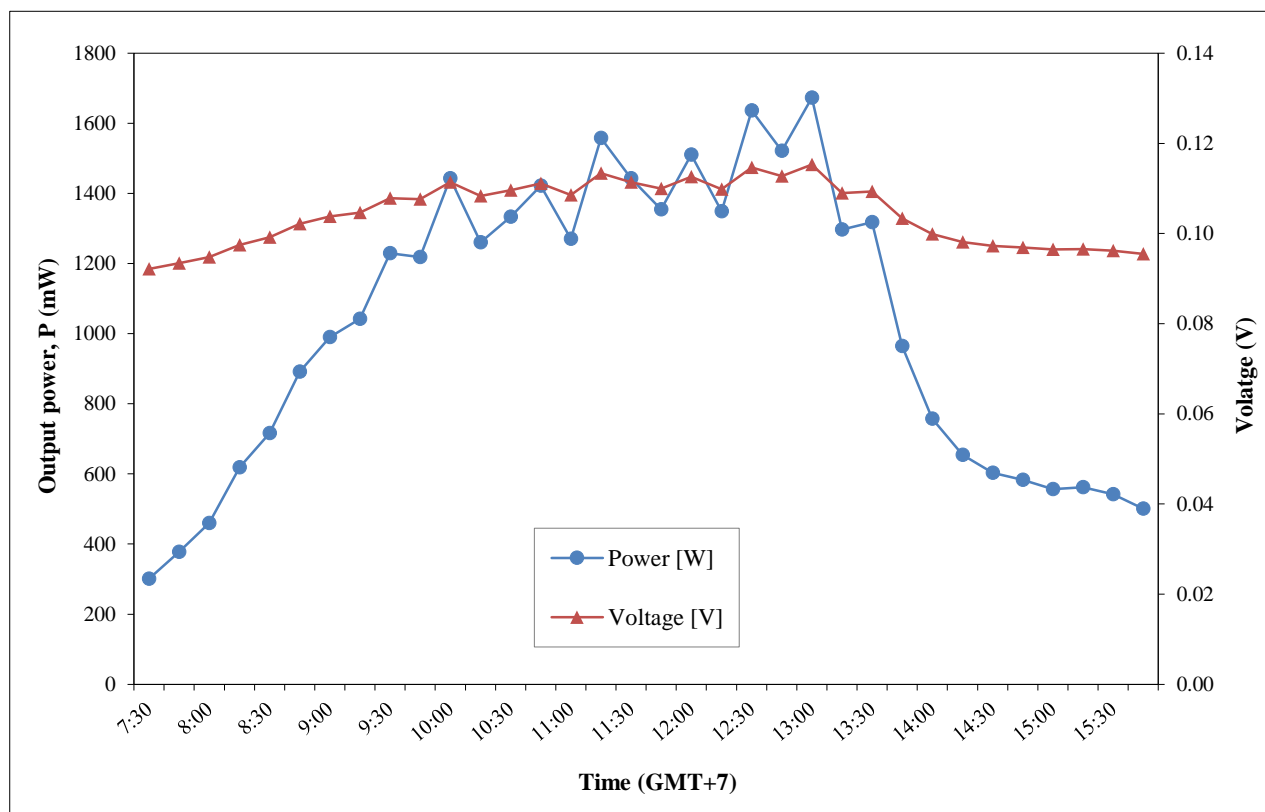


Figure 9. Output power and Voltage Thermoelectric

## 4. Conclusion

This paper describes the results of the investigation into the power output of the photovoltaic-thermoelectric generator. The combined system analysis of the two systems was conducted to increase the yield of electrical energy. Experimental studies are applied to the analysis of the output power and temperature distribution of photovoltaic systems. Exergy analysis is used to predict the performance of the combined system at low temperatures. The implementation of numerical analysis using software is applied to the generator thermoelectric model to determine system performance. This study shows the impact of the intensity of sunlight hitting the photovoltaic surface so that the surface of the panel experiences an increase in temperature and that affects energy efficiency. In addition, parametric studies on the effect of solar panel temperature on power in photovoltaic-thermoelectric systems have also been conducted. Based on the results and discussion, it can be concluded that thermoelectric can be used as a heat sink for photovoltaic by utilizing panel heat and increasing exergy efficiency due to the increased cooling effect. The results show that the highest temperature under the panel is 57°C at 1.00 PM. At 1.00 PM, the resulting power value is 39.8 W. Based on the bottom temperature of this panel, the Thermoelectric Generator can produce 1673.4 mW. The Photovoltaic-Thermoelectric Generator hybrid system resulted in a 4.2% increase. This system can be used in low-temperature conditions, but its performance needs improvement. Some of the findings in this study still have a lot of room for improvement. Therefore, future studies will attempt to investigate the effects of the shape of the thermoelectric leg, increasing the temperature difference on the thermoelectric, the use of nano-composites on the thermoelectric leg, and adding the cooling effect to the photovoltaic-thermoelectric system.

## 5. Declarations

### 5.1. Author Contributions

Conceptualization, C.H.; methodology, C.H., and E.R.; software, E.R.; validation, C.H.; formal analysis, C.H.; resources, T.T.; data curation, E.R., and T.T.; writing—original draft preparation, C.H.; writing—review and editing, E.R.; experimental setup, T.T.; structure design, T.T. All authors have read and agreed to the published version of the manuscript.

### 5.2. Data Availability Statement

The data presented in this study are available on request from the corresponding author.

### 5.3. Funding and Acknowledgements

The authors would like to thank the Universitas Sebelas Maret for laboratory facilities and financial assistance under the research grant project with contract number 254/UN27.22/PT.01.03/2022.

### 5.4. Conflicts of Interest

The authors declare no conflict of interest.

## 6. References

- [1] Harsito, C., Tjahjana, D.D.D.P., & Kristiawan, B. (2020). Savonius turbine performance with slotted blades. The 5<sup>th</sup> International Conference on Industrial, Mechanical, Electrical, And Chemical Engineering 2019 (ICIMECE 2019). doi:10.1063/5.0000797.
- [2] Tjahjana, D. D. D. P., Hadi, S., Wicaksono, Y. A., Kurniawati, D. M., Fahrudin, F., Utomo, I. S., ... & Prasetyo, A. (2019). Study on performance improvement of the Savonius wind turbine for Urban Power System with Omni-Directional Guide Vane (ODGV). *Journal of Advanced Research in Fluid Mechanics and Thermal Sciences*, 55(1), 126-135.
- [3] Tjahjana, D. D. D. P., Arifin, Z., Suyitno, S., Juwana, W. E., Prabowo, A. R., & Harsito, C. (2021). Experimental study of the effect of slotted blades on the Savonius wind turbine performance. *Theoretical and Applied Mechanics Letters*, 11(3), 100249. doi:10.1016/j.taml.2021.100249.
- [4] Ruzaimi, A., Shafie, S., Hassan, W. Z. W., Azis, N., Ya'Acob, M. E., & Supeni, E. E. (2019). Photovoltaic Panel Temperature and Heat Distribution Analysis for Thermoelectric Generator Application. 2018 IEEE 5<sup>th</sup> International Conference on Smart Instrumentation, Measurement and Application (ICSIMA). doi:10.1109/ICSIMA.2018.8688801.
- [5] Snyder, G. J., & Toberer, E. S. (2008). Complex thermoelectric materials. *Nature Materials*, 7(2), 105–114. doi:10.1038/nmat2090.
- [6] Beretta, D., Neophytou, N., Hodges, J. M., Kanatzidis, M. G., Narducci, D., Martin-Gonzalez, M., ... & Caironi, M. (2019). Thermoelectrics: From history, a window to the future. *Materials Science and Engineering: R: Reports*, 138, 100501. doi:10.1016/j.mser.2018.09.001.
- [7] Jaziri, N., Boughamoura, A., Müller, J., Mezghani, B., Tounsi, F., & Ismail, M. (2020). A comprehensive review of Thermoelectric Generators: Technologies and common applications. *Energy Reports*, 6, 264–287. doi:10.1016/j.egy.2019.12.011.
- [8] Talawo, R. C., Fotso, B. E. M., & Fogue, M. (2021). An experimental study of a solar thermoelectric generator with vortex tube for hybrid vehicle. *International Journal of Thermofluids*, 10(100079). doi:10.1016/j.ijft.2021.100079.
- [9] Xiao, J., Yang, T., Li, P., Zhai, P., & Zhang, Q. (2012). Thermal design and management for performance optimization of solar thermoelectric generator. *Applied Energy*, 93, 33–38. doi:10.1016/j.apenergy.2011.06.006.
- [10] Suzuki, R. O., Ito, K. O., & Oki, S. (2016). Analysis of the Performance of Thermoelectric Modules Under Concentrated Radiation Heat Flux. *Journal of Electronic Materials*, 45(3), 1827–1835. doi:10.1007/s11664-015-4237-z.
- [11] Li, G., Pei, G., Ji, J., Yang, M., Su, Y., & Xu, N. (2015). Numerical and experimental study on a PV/T system with static miniature solar concentrator. *Solar Energy*, 120, 565–574. doi:10.1016/j.solener.2015.07.046.
- [12] Da, Y., Xuan, Y., & Li, Q. (2016). From light trapping to solar energy utilization: A novel photovoltaic-thermoelectric hybrid system to fully utilize solar spectrum. *Energy*, 95, 200–210. doi:10.1016/j.energy.2015.12.024.
- [13] Makki, A., Omer, S., Su, Y., & Sabir, H. (2016). Numerical investigation of heat pipe-based photovoltaic-thermoelectric generator (HP-PV/TEG) hybrid system. *Energy Conversion and Management*, 112, 274–287. doi:10.1016/j.enconman.2015.12.069.
- [14] Cui, T., Xuan, Y., & Li, Q. (2016). Design of a novel concentrating photovoltaic-thermoelectric system incorporated with phase change materials. *Energy Conversion and Management*, 112, 49–60. doi:10.1016/j.enconman.2016.01.008.

- [15] Lamba, R., & Kaushik, S. C. (2016). Modeling and performance analysis of a concentrated photovoltaic-thermoelectric hybrid power generation system. *Energy Conversion and Management*, 115, 288–298. doi:10.1016/j.enconman.2016.02.061.
- [16] Zhu, W., Deng, Y., Wang, Y., Shen, S., & Gulfam, R. (2016). High-performance photovoltaic-thermoelectric hybrid power generation system with optimized thermal management. *Energy*, 100, 91–101. doi:10.1016/j.energy.2016.01.055.
- [17] Ju, X., Wang, Z., Flamant, G., Li, P., & Zhao, W. (2012). Numerical analysis and optimization of a spectrum splitting concentration photovoltaic-thermoelectric hybrid system. *Solar Energy*, 86(6), 1941–1954. doi:10.1016/j.solener.2012.02.024.
- [18] Elsarrag, E., Pernau, H., Heuer, J., Roshan, N., Alhorr, Y., & Bartholomé, K. (2015). Spectrum splitting for efficient utilization of solar radiation: a novel photovoltaic–thermoelectric power generation system. *Renewables: Wind, Water, and Solar*, 2(1). doi:10.1186/s40807-015-0016-y.
- [19] Zhang, J., & Xuan, Y. (2017). Performance improvement of a photovoltaic - Thermoelectric hybrid system subjecting to fluctuant solar radiation. *Renewable Energy*, 113, 1551–1558. doi:10.1016/j.renene.2017.07.003.
- [20] Zhang, X., Chau, K., & Chan, C. (2009). Design and Implementation of a Thermoelectric- Photovoltaic Hybrid Energy Source for Hybrid Electric Vehicles. *World Electric Vehicle Journal*, 3(2), 271–281. doi:10.3390/wevj3020271.
- [21] Jun, Y. J., Park, K. S., & Song, Y. H. (2021). A study on the structure of Solar/Photovoltaic Hybrid system for the purpose of preventing overheat and improving the system performance. *Solar Energy*, 230, 470–484. doi:10.1016/j.solener.2021.10.019.
- [22] Okpalike, C., Okeke, F. O., Ezema, E. C., Oforji, P. I., & Igwe, A. E. (2022). Effects of Renovation on Ventilation and Energy Saving in Residential Building. *Civil Engineering Journal*, 7, 124–134. doi:10.28991/cej-sp2021-07-09.
- [23] Maduabuchi, C., Lamba, R., Njoku, H., Eke, M., & Mgbemene, C. (2021). Effects of leg geometry and multistaging of thermoelectric modules on the performance of a photovoltaic-thermoelectric system using different photovoltaic cells. *International Journal of Energy Research*, 45(12), 17888–17902. doi:10.1002/er.6925.
- [24] Erturun, U., & Mossi, K. (2012). A Feasibility Investigation on Improving Structural Integrity of Thermoelectric Modules With Varying Geometry. Volume 2: Mechanics and Behavior of Active Materials; Integrated System Design and Implementation; Bio-Inspired Materials and Systems; Energy Harvesting. doi:10.1115/smasis2012-8247.
- [25] Ruzaimi, A., Shafie, S., Hassan, W. Z. W., Azis, N., Effendy Ya'acob, M., & Elianddy, E. (2020). Temperature distribution analysis of monocrystalline photovoltaic panel for photovoltaic-thermoelectric generator (PV-TEG) hybrid application. *Indonesian Journal of Electrical Engineering and Computer Science*, 17(2), 858–867. doi:10.11591/ijeecs.v17.i2.pp858-867.
- [26] Doraghi, Q., Khordehgah, N., Żabnieńska-Góra, A., Ahmad, L., Norman, L., Ahmad, D., & Jouhara, H. (2021). Investigation and computational modelling of variable teg leg geometries. *ChemEngineering*, 5(3), 1–16. doi:10.3390/chemengineering5030045.
- [27] Ibeagwu, O. I. (2019). Modelling and comprehensive analysis of TEGs with diverse variable leg geometry. *Energy*, 180, 90–106. doi:10.1016/j.energy.2019.05.088.